

Supplementary data

Inventory of Supplementary Information

Supplementary Figures and Figure Legends

Supplementary Tables

Table S1. Primers used for qRT–PCR, MeRIP–qPCR and RIP–qPCR assay.

Table S2. Primers used for vector construction.

Table S3. Antibodies used in this study.

Table S4. GO of m⁶A downregulated peaks.

Table S5. GO of upregulated genes in RNA–seq.

Table S6. GO of downregulated genes in RNA–seq.

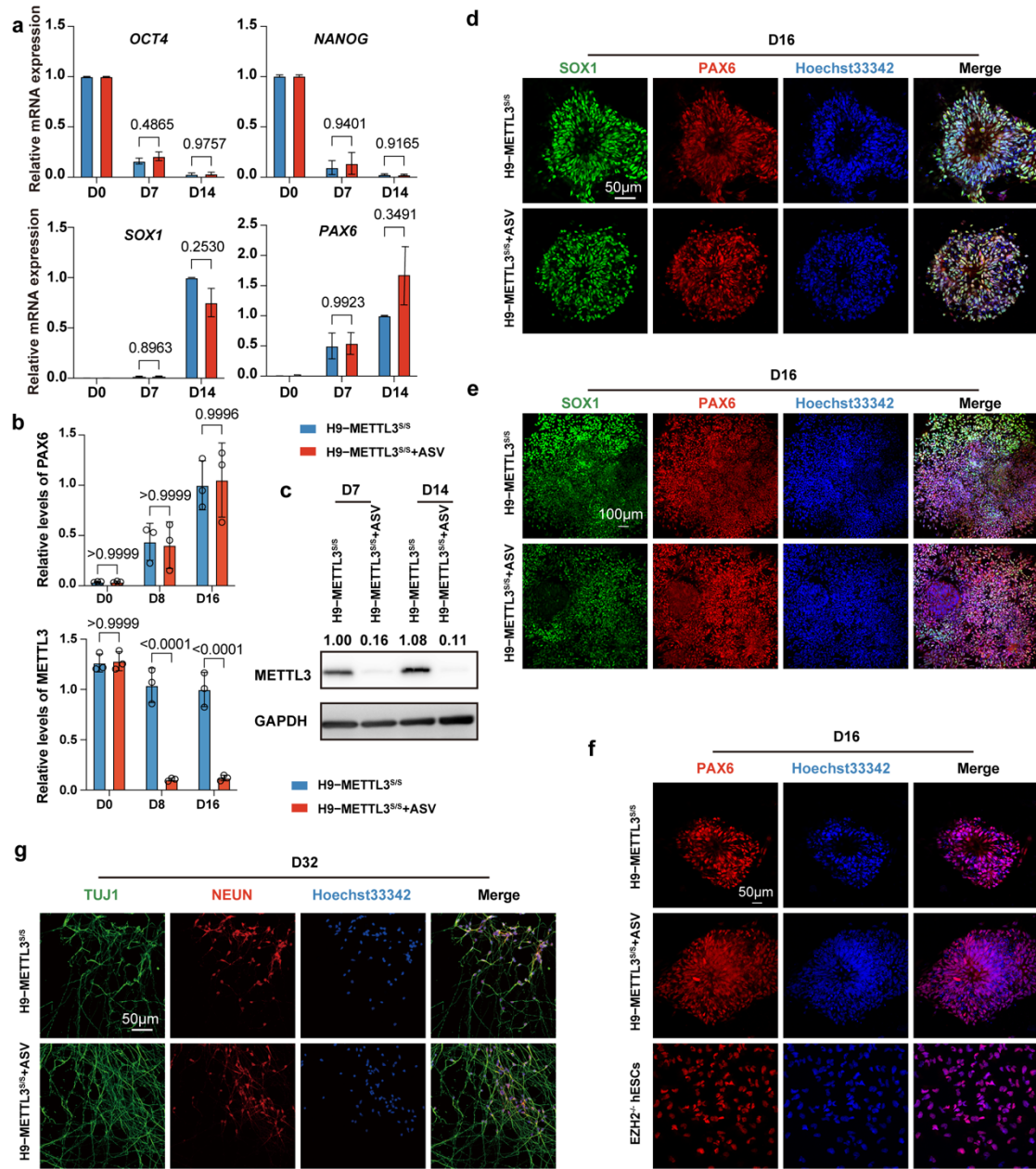


Figure S1. NPC differentiation and neuron differentiation of METTL3^{s/s} hESCs using EB method. **(a)** qRT-PCR analysis on the expression level of the pluripotent genes (*NANOG* and *OCT4*) and the hNPC genes (*PAX6* and *SOX1*) in H9-METTL3^{s/s} hESCs and H9-METTL3^{s/s} hESCs after ASV treatment at day 0, day 7 and day 14 of neural differentiation. H9-METTL3^{s/s} hESCs serve as control. Data represent mean \pm SD ($n = 3$, two-way ANOVA). **(b)** Relative intensities analysis of western blot in Figure 2c. **(c)** Western blot of H9-METTL3^{s/s} hESCs and H9-METTL3^{s/s} hESCs after ASV treatment for METTL3 at day 7 and day 14 of neural differentiation. GAPDH was

probed as an internal loading control. (d) Immunostaining images of H9–METTL3^{s/s} hESCs and H9–METTL3^{s/s} hESCs after ASV treatment for SOX1 (green) and PAX6 (red) at day 16 of neural differentiation. Scale bar, 50 μm . (e) Immunostaining images show the rosette-like morphology of H9–METTL3^{s/s} hESCs and H9–METTL3^{s/s} hESCs after ASV treatment for SOX1 (green) and PAX6 (red) at day 16 of neural differentiation. Scale bar, 100 μm . (f) Immunostaining images show the rosette-like morphology of H9–METTL3^{s/s} hESCs, H9–METTL3^{s/s} hESCs after ASV treatment and EZH2^{-/-} hESCs (negative control) at day 16 of neural differentiation. Scale bar, 50 μm . (g) Immunostaining images of H9–METTL3^{s/s} hNPCs and H9–METTL3^{s/s} hNPCs after ASV treatment for TUJ1 (green) and NEUN (red) at day 32 of neural differentiation. Scale bar, 50 μm .

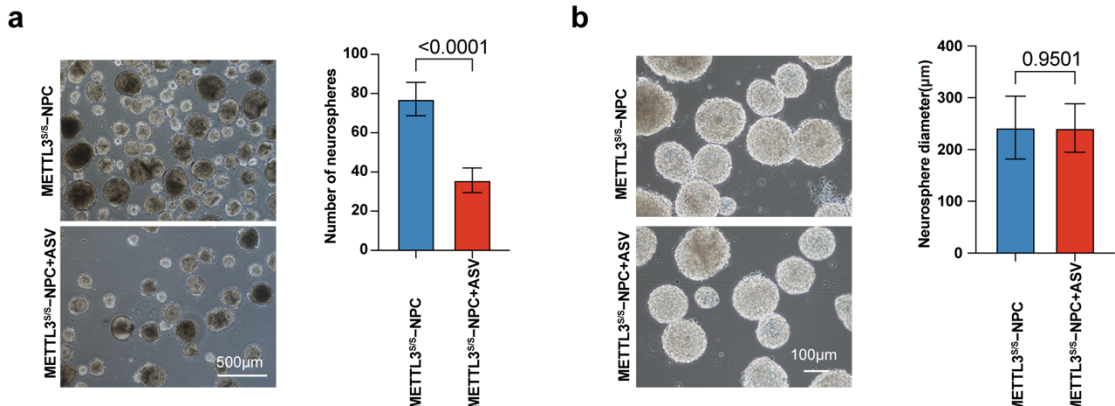


Figure S2. Characterization of METTL3^{s/s} hNPCs using EB method. **(a)** The number of neurospheres in METTL3^{s/s} hNPCs and METTL3^{s/s} hNPCs after ASV treatment. **(b)** The diameter of neurospheres in METTL3^{s/s} hNPCs and METTL3^{s/s} hNPCs after ASV treatment.

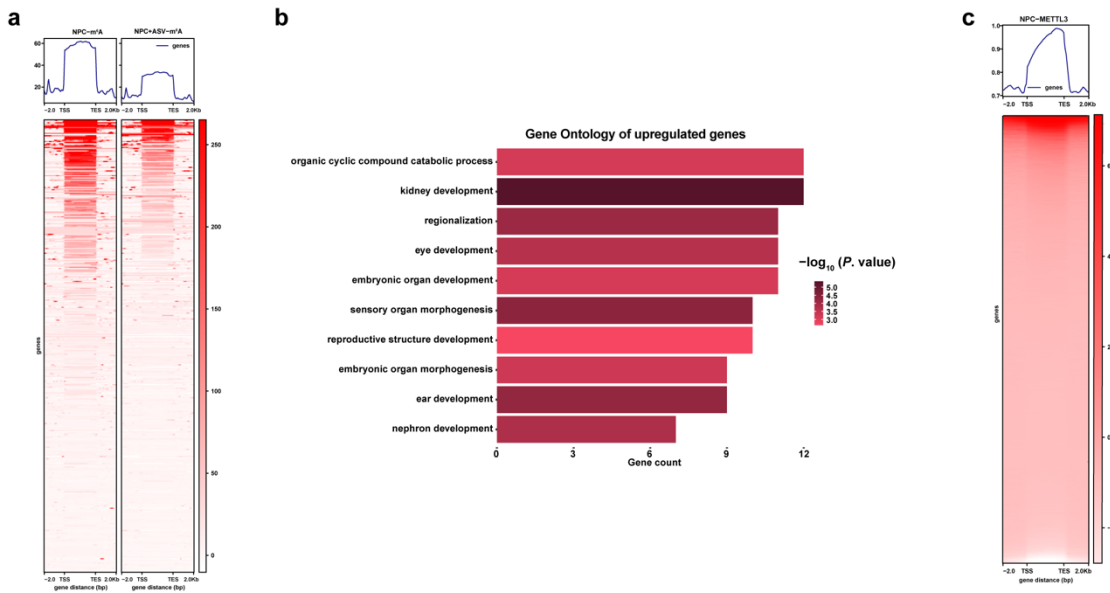


Figure S3. Bioinformatic outcomes of METTL3^{s/s} hNPCs with or without ASV. **(a)** The heatmap of m⁶A peaks in METTL3^{s/s} hNPCs and METTL3^{s/s} hNPCs after ASV treatment. **(b)** Gene Ontology (GO) analysis for upregulated genes in H9-METTL3^{s/s} hNPCs after ASV treatment. **(c)** The heatmap of METTL3 peaks in H9-METTL3^{s/s} hNPCs.

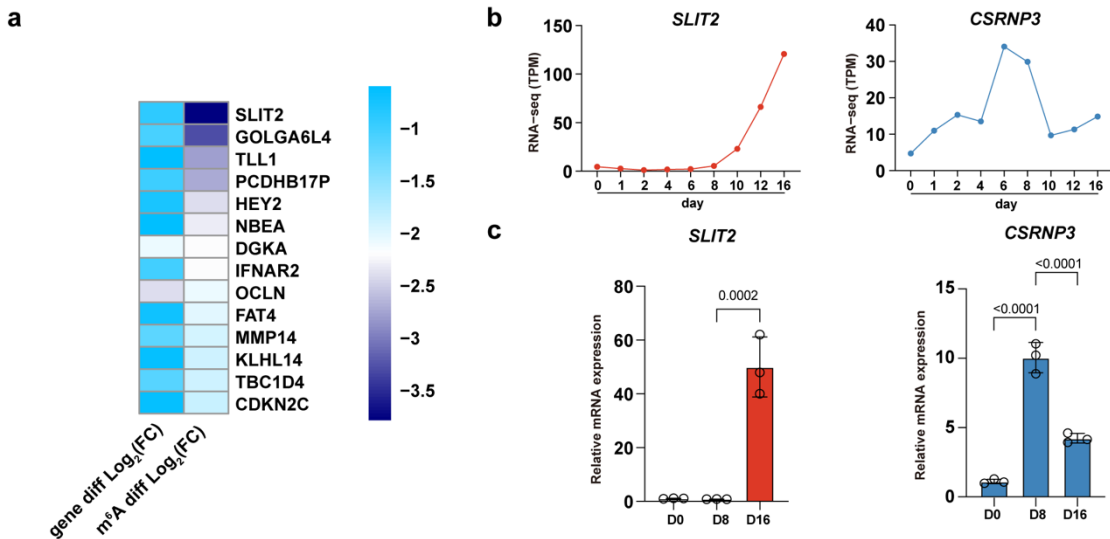


Figure S4. SLIT2 is the key gene associated with hNPCs proliferation. **(a)** The heatmap of top genes in m⁶A differential genes and differential expression genes in METTL3^{s/s} hNPCs and METTL3^{s/s} hNPCs after ASV treatment. **(b)** The expression of *CSRNP3* and *SLIT2* in time-course RNA-seq. **(c)** qRT-PCR analysis on the expression level of *CSRNP3* and *SLIT2* in H9-METTL3^{s/s} hESCs at day 0, day 8 and day 16 of neural differentiation. H9-METTL3^{s/s} hESCs serve as control. Data represent mean \pm SD ($n = 3$, two-way ANOVA).

Supplementary Tables

Table S1. Primers used for RT–qPCR, MeRIP–qPCR and RIP–qPCR assay.

hGAPDH-qF	ATGACATCAAGAAGGTGGTG	RT–qPCR
hGAPDH-qR	CATACCAGGAAATGAGCTTG	RT–qPCR
hOCT4-qF	ACATCAAAGCTCTGCAGAAA GAACT	RT–qPCR
hOCT4-qR	CTGAATACCTTCCCAAATAGA ACCC	RT–qPCR
hNANOG-qF	ATTCTTCCACCAGTCCAAA	RT–qPCR
hNANOG-qR	ATCTGCTGGAGGCTGAGGTA	RT–qPCR
hSOX1-qF	AATTTTATTTCGGCGTTGC	RT–qPCR
hSOX1-qR	TGGGCTCTGTCTCTTAAATT GT	RT–qPCR
hPAX6-qF	TCTTGCTTGGGAAATCCG	RT–qPCR
hPAX6-qR	CTGCCCGTTAACATCCTTAG	RT–qPCR
qh-SLIT2-F2	AGCTTAGACGAATTGACCTG AGC	RT–qPCR
qh-SLIT2-R2	CCGAAGGCAGTTATCTTGGT GG	RT–qPCR
qh-CSRNP3-F1	CTGTGACTGCCGAGTGTCT	RT–qPCR
qh-CSRNP3-R1	ACATACGATCCACCTGGCAC	RT–qPCR
MeRIP-qPCR-SLI T2-F	TGGGAACCATTGCAACTCGG G	MeRIP-qPCR&RIP-q PCR
MeRIP-qPCR-SLI T2-R	AGCTCCTCTGTCCCTCGTGC	MeRIP-qPCR&RIP-q PCR

Table S2. Primers used for vector construction.

METTL3-sg RNA-3-Olig o1	CACCGTATGGATTCTTAGCTCTGTA
METTL3-sg RNA-3-Olig o2	AAACTACAGAGCTAAGAATCCATAC
METTL3-H L-F2	GATCTTCCGGATGGCGTGAGCAGGTTGGTGTCAAAG
METTL3-H L-R	TATGGGTATAAATTCTTAGGTTAGAGATGATACCATCTGG
METTL3-H R-F1	ATAACTTCGTATAATGTATGCTATACGAAGTTATAAGCACTTCC TTACAGAGCTAAG
METTL3-H R-R2	ATTGTAGGAGATCTTGTGGTGGGTTGAAGAAACTTGTG
PURO-F1	GTACTAAATAACTCGTATAATGTATGCTATACGAAGTTATTAC CGGGTAGGGGAGGCAGC
PGK-R1	ACATTATACGAAGTTATCAGGCAGGGAGGCAGGCCAAAGGGA G
SMASh-F1	GAATTTATACCCATACGATGTTCCAGATTACGCTTATCCCTACG ACGTGCCTGATTATGCATACCCATATGATG
SMASh-F2	GATTATGCATACCCATATGATGTCCCCGACTATGCCGACGAGA TGGAGGAGTGTCCCCAG

Table S3. Antibodies used in this study.

Antibodies	Manufacture	Catalog
METTL3 antibody	Abcam (Cambridge, MA, USA)	ab195352
SOX1 antibody	R&D system (Minneapolis, MN, USA)	AF3369
PAX6 antibody	Biolegend (San Diego, CA, USA)	901301
MAP2 antibody	Abcam (Cambridge, MA, USA)	ab32454
SOX2 antibody	R&D system (Minneapolis, MN, USA)	AF2018
NEUN antibody	Milipore (Boston, MA, USA)	ABN78
TUJ-1 antibody	Biolegend (San Diego, CA, USA)	801201
m ⁶ A antibody	Abcam (Cambridge, MA, USA) /Synaptic Systems (German)	ab286164 /202203
Rabbit IgG	CST (Boston, CA, USA)	2729
Donkey anti-Goat IgG (H+L) Cross-Adsorbed Secondary Antibody, Alexa Fluor™ 488	Invitrogen (Carlsbad, CA, USA)	A11055
Donkey anti-Goat IgG (H+L) Cross-Adsorbed Secondary Antibody, Alexa Fluor™ 594	Invitrogen (Carlsbad, CA, USA)	A11058
Donkey anti-Rabbit IgG (H+L) Cross-Adsorbed Secondary Antibody, Alexa Fluor™ 488	Invitrogen (Carlsbad, CA, USA)	A11008
Donkey anti-Rabbit IgG (H+L) Cross-Adsorbed Secondary Antibody, Alexa Fluor™ 594	Invitrogen (Carlsbad, CA, USA)	A11012
Anti-rabbit IgG, HRP-linked Antibody	CST (Boston, CA, USA)	7074s

Table S4. GO of m⁶A downregulated peaks.

ID	Description	pvalue	Count
GO:0008380	RNA splicing	9.11E-16	68
GO:0022613	ribonucleoprotein complex biogenesis	6.96E-12	63
GO:0016570	histone modification	2.20E-08	55
GO:0140694	non-membrane-bounded organelle assembly	1.12E-10	52
GO:0048285	organelle fission	7.63E-06	50
GO:0000280	nuclear division	1.96E-06	48
GO:0006325	chromatin organization	6.15E-07	47
GO:0044772	mitotic cell cycle phase transition	1.71E-06	47
GO:0006260	DNA replication	5.66E-13	46
GO:0007346	regulation of mitotic cell cycle	5.67E-05	45
GO:0006417	regulation of translation	0.00128771	41
GO:0050808	synapse organization	0.00038446	40
GO:0010975	regulation of neuron projection development	0.00513974	37
GO:0061564	axon development	0.01736094	36
GO:0030900	forebrain development	0.00218787	34

Table S5. GO of upregulated genes in RNA-seq.

ID	Description	pvalue	Count
GO:0001822	kidney development	4.35E-06	12
GO:1901361	organic cyclic compound catabolic process	0.00065042	12
GO:0003002	regionalization	7.49E-05	11
GO:0001654	eye development	0.00020362	11
GO:0048568	embryonic organ development	0.00066608	11
GO:0090596	sensory organ morphogenesis	4.19E-05	10
GO:0048608	reproductive structure development	0.00223968	10
GO:0043583	ear development	5.60E-05	9
GO:0048562	embryonic organ morphogenesis	0.00049445	9
GO:0072006	nephron development	0.00014847	7

Table S6. GO of downregulated genes in RNA-seq.

ID	Description	pvalue	Count
GO:0007389	pattern specification process	7.24E-10	27
GO:0061564	axon development	5.32E-07	23
GO:0034329	cell junction assembly	8.50E-07	22
GO:0030900	forebrain development	6.08E-06	19
GO:0050808	synapse organization	3.11E-05	19
GO:0016055	Wnt signaling pathway	0.00016201	18
GO:0050673	epithelial cell proliferation	0.00016753	17
GO:0030111	regulation of Wnt signaling pathway	0.00022437	15
GO:0050678	regulation of epithelial cell proliferation	0.00040783	15
GO:0030198	extracellular matrix organization	0.00078352	14
GO:0031589	cell–substrate adhesion	0.00102055	14
GO:0010631	epithelial cell migration	0.00141276	13
GO:0043410	positive regulation of MAPK cascade	0.00339217	13
GO:0098742	cell–cell adhesion via plasma–membrane adhesion molecules	0.01021831	12
GO:0050767	regulation of neurogenesis	0.03291139	12